

FINAL
IN 34-12
OCT
014783**DEVELOPMENT OF A LOW-REYNOLDS NUMBER, NONLINEAR k - ϵ MODEL FOR THE REDUCED NAVIER-STOKES EQUATIONS**

A Final Technical Report for NASA-LeRC Grant NAG-1781

David A. Boger*, T.R. Govindan**, and Henry McDonald***
The Pennsylvania State University
The Applied Research Laboratory**I. INTRODUCTION**

Previous work at NASA LeRC has shown that flow distortions in aircraft engine inlet ducts can be significantly reduced by mounting vortex generators, or small wing sections, on the inside surface of the engine inlet [1]. The placement of the vortex generators is an important factor in obtaining the optimal effect over a wide operating envelope. In this regard, the only alternative to a long and expensive test program which would search out this optimal configuration is a good prediction procedure which could narrow the field of search. Such a procedure has been developed in collaboration with NASA LeRC, and results obtained by NASA personnel indicate that it shows considerable promise for predicting the viscous turbulent flow in engine inlet ducts in the presence of vortex generators [1].

The prediction tool is a computer code which numerically solves the reduced Navier-Stokes equations and so is commonly referred to as RNS3D. Obvious deficiencies in RNS3D have been addressed in previous work [3]. Primarily, it is known that the predictions of the mean velocity field of a turbulent boundary layer flow approaching separation are not in good agreement with data [1]. It was suggested that the use of an algebraic mixing-length turbulence model in RNS3D is at least partly to blame for this. Additionally, the current turbulence model includes an assumption of isotropy which will ultimately fail to capture turbulence-driven secondary flow known to exist in noncircular ducts [30].

Because turbulent flows contain time and length scales which can vary dramatically, it is widely acknowledged that two-equation turbulence models represent the minimum acceptable level of closure for general modeling [31]. Such a model must also have the capability to integrate the solution all the way to the wall, since flows containing vortex generators will be highly dependent on the structure of the turbulence in the near-wall region. Recent work has also demonstrated that an anisotropic eddy viscosity, in conjunction with a two-equation turbulence model, will significantly enhance the prediction of anisotropic effects [30].

For these reasons, the current effort was undertaken to incorporate a low-Reynolds number, anisotropic k - ϵ model directly into the RNS3D code, so that the improved modeling capability demonstrated in previous work would be accessible for internal flows without sacrificing any of the efficiency which RNS3D makes available to its users.

* Research Assistant, Fluid Dynamics & Turbomachinery Dept.

** Sr. Research Associate, Computational Mechanics Dept.

*** Assistant Director, Computational Sciences. Presently Director, NASA Ames Research Center

II. LOW-REYNOLDS NUMBER TURBULENCE MODELING

The Governing Equations

In this work, the two-equation turbulence model based on the turbulent kinetic energy, k , and the turbulent energy dissipation rate, ϵ , was developed, implemented, and tested within the context of the reduced Navier-Stokes equations as they appear in the RNS3D code. While many variations of two-equation turbulence models exist, the k - ϵ formulation has the distinct advantage of having been widely used and studied over the longest period of time.

As with the algebraic mixing-length model, the two-equation model provides for an eddy viscosity which is based on characteristic length and velocity scales of the turbulence. In this case, the velocity scale is determined by the square root of the turbulent kinetic energy, for which a transport equation can be derived exactly from the Navier-Stokes equations using Reynolds-averaging. The resulting equation, once some modeling is completed, can be written

$$\rho \frac{\partial k}{\partial t} + \rho U_j \frac{\partial k}{\partial x_j} = \frac{\partial}{\partial x_j} \left[\left(\mu + \frac{\mu_t}{\sigma_k} \right) \frac{\partial k}{\partial x_j} \right] - \rho \overline{u_i u_j} \frac{\partial U_i}{\partial x_j} - \rho \epsilon - D. \quad (1)$$

Here, the time rate of change and convection terms, which appear on the left-hand side of the equation, are captured exactly, as are the molecular diffusion, production and dissipation terms which appear on the right. Turbulent diffusion effects, which appear as a factor of the turbulent viscosity, μ_t , are approximated by a gradient-diffusion assumption from which the empirical coefficient σ_k arises. Finally, the term represented by D arises from near-wall modeling and typically takes the value of the dissipation at the wall [14].

The characteristic length scale of the turbulence can be derived from the ratio

$$l = k^{3/2} / \epsilon \quad (2)$$

although a transport equation for ϵ is comparatively more difficult to obtain. Exact equations can be derived from the momentum disturbance equations or for enstrophy, the averaged magnitude of the fluctuating vorticity, which approaches the dissipation rate for high Reynolds numbers. A practical model can then be deduced through order-of-magnitude and dimensional arguments. The final form is fairly well-established, and can be written

$$\rho \frac{\partial \epsilon}{\partial t} + \rho U_j \frac{\partial \epsilon}{\partial x_j} = \frac{\partial}{\partial x_j} \left[\left(\mu + \frac{\mu_t}{\sigma_\epsilon} \right) \frac{\partial \epsilon}{\partial x_j} \right] - C_{\epsilon 1} \frac{\epsilon}{k} \rho \overline{u_i u_j} \frac{\partial U_i}{\partial x_j} - C_{\epsilon 2} \rho \frac{\epsilon^2}{k} - E. \quad (3)$$

Three empirical coefficients appear in the equation for the turbulent energy dissipation, and they are represented by $C_{\epsilon 1}$, $C_{\epsilon 2}$, and σ_ϵ . The term E arises from near-wall modeling, but is typically ad-hoc in nature [14].

Usually, the Reynolds stresses are represented by the Boussinesq approximation,

$$-\rho \overline{u_i u_j} = -\frac{2}{3} \rho k \delta_{ij} + 2\mu_t E_{ij}, \quad (4)$$

where the mean strain rate tensor, E_{ij} , is defined as

$$E_{ij} = \frac{1}{2} \left(\frac{\partial U_i}{\partial x_j} + \frac{\partial U_j}{\partial x_i} \right). \quad (5)$$

The eddy viscosity, in the k - ϵ formulation, is determined by

$$\mu_t = \rho C_\mu \frac{k^2}{\epsilon}, \quad (6)$$

in which C_μ is an empirical constant.

Under the RNS3D assumptions, the streamwise diffusion terms were neglected from both equations [4]. Incorporating the RNS3D coordinate system and linearizing the equations then gives

$$\begin{aligned} \frac{\rho \mu_p}{h} \frac{\partial \hat{k}}{\partial x_3} + \rho v_s \frac{\partial \hat{k}}{\partial x_1} + \rho w_s \frac{\partial \hat{k}}{\partial x_2} &= \frac{1}{Re} \frac{1}{h} \frac{\partial}{\partial x_1} \left[h \left(\mu + \frac{\mu_t}{\sigma_k} \right) \frac{\partial \hat{k}}{\partial x_1} \right] \\ &+ \frac{1}{Re} \frac{1}{h} \frac{\partial}{\partial x_2} \left[h \left(\mu + \frac{\mu_t}{\sigma_k} \right) \frac{\partial \hat{k}}{\partial x_2} \right] + \frac{\mu_t}{Re} \Phi - \rho \hat{\epsilon} - D \end{aligned} \quad (7)$$

for the k -equation, where a hat denotes an implicitly treated variable. The production term, which depends on Φ , the strain-rate invariant, and the low-Reynolds number function D were both treated explicitly. Similarly, the ϵ -equation is given by

$$\begin{aligned} \frac{\rho \mu_p}{h} \frac{\partial \hat{\epsilon}}{\partial x_3} + \rho v_s \frac{\partial \hat{\epsilon}}{\partial x_1} + \rho w_s \frac{\partial \hat{\epsilon}}{\partial x_2} &= \frac{1}{Re} \frac{1}{h} \frac{\partial}{\partial x_1} \left[h \left(\mu + \frac{\mu_t}{\sigma_\epsilon} \right) \frac{\partial \hat{\epsilon}}{\partial x_1} \right] \\ &+ \frac{1}{Re} \frac{1}{h} \frac{\partial}{\partial x_2} \left[h \left(\mu + \frac{\mu_t}{\sigma_\epsilon} \right) \frac{\partial \hat{\epsilon}}{\partial x_2} \right] + \rho C_{\epsilon 1} C_\mu \Phi \hat{k} + \rho C_{\epsilon 2} \left(\frac{\epsilon}{k} \right)^2 \hat{k} - 2\rho C_{\epsilon 2} \left(\frac{\epsilon}{k} \right) \hat{\epsilon} - E \end{aligned} \quad (8)$$

where, once again, the hatted variables denote those which are treated implicitly. The linearization of the destruction term here is borrowed from that used in previous studies, where it was found to be successful. The low-Reynolds number function E is treated explicitly.

The Low-Reynolds Number Modifications

Despite success with the Launder-Sharma modifications [18] in previous studies [3], it was found that the low-Reynolds number function E suggested by Launder-Sharma, when modified according to the assumptions in RNS3D, became unstable. For this reason, the low-Reynolds number modifications of Chien were adopted [5]. These modifications consisted of the functions

$$D = 2\nu k / y^2, \quad (9)$$

which models the wall value of ϵ , allowing the boundary condition on ϵ to be zero, and

$$E = (2\nu\epsilon / y^2)\exp(-0.5y^+), \quad (10)$$

which also models a "wall" dissipation effect. Damping functions multiply the empirical constants C_μ and $C_{\epsilon 2}$. They are

$$f_\mu = 1 - \exp(-0.0115y^+) \quad (11)$$

for the damping of the eddy viscosity, and

$$f_2 = 1 - (2/9)\exp[-(R_T/6)^2], \quad (12)$$

which decreases the destruction of dissipation in the near-wall region. Note that, because the functions depend on both the distance to the wall, y , and the normalized distance to the wall, y^+ , the normal distance to the wall, as well as the friction velocity at the wall, must be calculated. Five empirical constants appear in the model. They are set, according to Chien [5], as

$$C_\mu = 0.09, \quad C_{\epsilon 1} = 1.35, \quad C_{\epsilon 2} = 1.8, \quad \sigma_k = 1.0, \quad \sigma_\epsilon = 1.3. \quad (13)$$

Initial Values

Equations (5)-(13) describe a coupled system of equations which can be solved within the RNS3D code by streamwise marching. Thus, in addition to boundary conditions, for example, at the wall, a complete description of the turbulent quantities are needed at the inlet of the duct. In this study, the values obtained by the existing mixing-length model at the first streamwise station are utilized to obtain initial profiles for k and ϵ . The approach taken is equivalent to that used in deriving wall-functions for the two variables. That is, it is assumed that production is equal to dissipation throughout the inlet plane, allowing k and ϵ to be derived from the mixing length eddy viscosity. The resulting equation for k is

$$k = C_\mu^{-1/2} l^2 \Phi \quad (14)$$

where l is the turbulent mixing length and Φ is the strain-rate invariant, and

$$\epsilon = C_\mu^{3/4} k^{3/2} / l. \quad (15)$$

Previous experience has shown the utility of damping C_μ in accordance with the low-Reynolds number modifications. In this work, the damping on the initial plane was based on the function of Launder-Sharma [18],

$$f_{\mu} = \exp[-3.4/(1+R_T/50)^2] \quad (16)$$

where R_T , the turbulent Reynolds number, is based on the mixing length eddy viscosity,

$$R_T = \frac{\rho l^2 \sqrt{\Phi}}{\mu C_{\mu}}. \quad (17)$$

When Eq. (17) is substituted into Eq. (16), the implicit relation

$$C_{\mu} = 0.09 \exp\{-3.4 / [1 + \rho l^2 \sqrt{\Phi} / (50 \mu C_{\mu})]^2\} \quad (18)$$

is obtained. In this work, Eq. (18) was solved using no more than three or four iterations of Newton's method.

Validation

Chien's model [5], as described, was implemented directly into the RNS3D code, borrowing heavily from the coding of the stream function-vorticity equations. That is, the k and ϵ equations were coupled and solved using the 2x2 alternating-direction implicit (ADI) solver which was already in place.

Initial solutions were obtained in a straight, circular duct at a Reynolds number of 150,000 and compared with expected near-wall behaviors. The results are shown in Figures 1 and 2, attached at the end of this report. Figure 1 shows the fully-developed velocity profile for the circular pipe flow. It can be seen that the viscous sublayer and buffer layer are captured well, though the logarithmic region has a slope and intercept which may be slightly different than expected. Figure 2 shows the turbulent kinetic energy scaled by the friction velocity squared. Its near-wall behavior is again as expected and fits between the empirical bounds. In the logarithmic region, the turbulent kinetic energy levels off to a near-constant value; however, the value attained is slightly higher than what is typically expected.

An extensive review of solutions of this type is available by Hreynya, et. al. [11].

III. ANISOTROPIC TURBULENCE MODELING

Two-equation turbulence models, especially those which depend on k and ϵ , have become popular for modern engineering applications of computational fluid dynamics. They are more general than algebraic mixing-length models and are much less computationally expensive than full Reynolds stress models (*i.e.*, those which model and solve each component of the Reynolds stress tensor separately). One drawback, however, is the assumption of an isotropic eddy viscosity, which causes the normal Reynolds stresses in most cases to be roughly, but erroneously, equal.

As early as 1957, Rivlin had noted the potential importance of normal Reynolds stress differences [24]. Rivlin compared turbulent with non-Newtonian, visco-elastic flows in a non-circular straight duct where both were characterized by secondary velocities in a plane normal to the primary flow direction. Noting that the secondary flow in the non-Newtonian fluid was generated by differences in normal stress, Rivlin suggested that differences in the normal Reynolds stresses might explain the secondary motion in turbulent flow. Several years later, Gessner and Jones showed experimentally that this was indeed the case [9]. Building on this work, researchers such as Lumley suggested that a nonlinear constitutive relation for the Reynolds stresses, comparable to that used for non-Newtonian fluids, might be appropriate [19]. These suggestions gave rise to two schools of nonlinear turbulence modeling in which researchers hoped to capture anisotropic effects with a nonlinear, or "anisotropic," eddy viscosity without resorting to the solution of six second-order, nonlinear, partial differential closure equations.

The first class of models, the "algebraic Reynolds stress models" (ARSM), such as that developed by Rodi (1976), are typically derived from the Reynolds stress equations by relating the transport of the Reynolds stress to the transport of the turbulent kinetic energy [25,26]. The result is an implicit, nonlinear, algebraic relation for the Reynolds stresses and is also a function of k and ϵ .

A second class of models, largely credited to Speziale (1987), has been termed the "nonlinear k - ϵ models" [30]. These models, though they have been derived in different ways by different investigators, all assume that the relationship between the Reynolds stress and the mean strain rate tensor is not linear but includes terms which are quadratic in the mean strain rate tensor as well. This idea, which provides an explicit relationship for the Reynolds stresses, is not new, but instead has been applied before in visco-elastic fluid dynamics and rarefied gas dynamics modeling [24,39].

It is only in the past few years that a clear understanding of the relationship between these two models was achieved in light of an exact explicit solution to Rodi's implicit model [8]. The so-called "explicit ARSM," then, may represent the state-of-the-art in anisotropic modeling and helps to clearly define the relationship among the algebraic models described above.

Implicit Algebraic Reynolds Stress Modeling

In deriving an implicit nonlinear stress-strain relation for the Reynolds stresses, τ_{ij} , Rodi [25,26] began with the exact equations for the Reynolds stresses and the turbulent kinetic energy and progressed with the assumption that their transport is proportional in the following way:

$$\text{Transport } (\tau_{ij}) \approx \frac{\tau_{ij}}{\rho k} \text{ Transport } (\rho k) \quad (19)$$

or, from their governing equations,

$$-P_{ij} + \epsilon_{ij} - \Pi_{ij} = \frac{\tau_{ij}}{\rho k} (P - \rho\epsilon), \quad (20)$$

where

$$P_{ij} = \tau_{ik} \frac{\partial U_j}{\partial x_k} + \tau_{jk} \frac{\partial U_i}{\partial x_k}, \quad P_{ii} = 2P. \quad (21)$$

Next, Rodi used Kolmogorov's hypothesis of local isotropy for the dissipation in which

$$\epsilon_{ij} \approx \frac{2}{3} \rho \epsilon \delta_{ij}. \quad (22)$$

The pressure strain can be broken into the sum of its slow and rapid parts if buoyancy and wall effects are neglected. For the slow pressure strain, Rotta's linear return-to-isotropy hypothesis (1972) was invoked, while for the rapid pressure strain, a model developed by Naot, Shavit, and Wolfshtein (1970) or W.C. Reynolds (1970) can be used [17]. The resulting model for the pressure strain has

$$\Pi_{ij} = C_1 \frac{\epsilon}{k} \left(\tau_{ij} + \frac{2}{3} \rho k \delta_{ij} \right) - \gamma \left(P_{ij} - \frac{2}{3} \delta_{ij} P \right) \quad (23)$$

where $1.4 \leq C_1 \leq 2.2$, and $.60 \leq \gamma \leq .78$.

The nonlinear model of Rodi is obtained by substituting Eqs. (22)-(23) into Eq. (20), which gives

$$\tau_{ij} = -\frac{2}{3} \rho k \delta_{ij} + \rho k (\gamma - 1) \left(P_{ij} - \frac{2}{3} P \delta_{ij} \right) / \left[P - \rho \epsilon (1 - C_1) \right]. \quad (24)$$

Typically, this implicit model is implemented by lagging the production, P , and then inverting the linear system of equations for the Reynolds stress components.

The model gives improved results for the square duct problem, where turbulence-driven secondary flow is induced [6,26], and has been a popular improvement in flows which contain swirl or rotational effects [2,15,34].

Nonlinear k - ϵ Modeling

Despite some success with the implicit ARSM, some researchers have complained that the model is based on "drastic assumptions which have not yet been verified" [21], while others added that the implicit model is "cumbersome to implement in complex flows" and that "numerical stiffness problems can result from the need for successive matrix inversions at each iteration" [8]. Thus, an explicit nonlinear model was sought.

Assuming that the Boussinesq approximation represents only the leading terms of a series

expansion about the strain rate, Speziale derived a nonlinear k - ϵ model by means of a quadratic expansion subject to physical constraints such as dimensional and tensorial invariance, realizability, and material frame-indifference [30]. Independently, Yoshizawa used a multiscale Direct-Interaction Approximation to develop a nonlinear k - ϵ model which included thermal buoyancy effects and an anisotropic model for turbulent heat flux as well [35,36]. Several subsequent works refined these models (including the addition of near-wall modifications) using two- and three-dimensional channel flows [20,21,22,23,27]. More recently, Shih and Lumley developed a nonlinear k - ϵ model, again using an expansion through terms quadratic in the strain rate and subjecting it to constraints which make it fully realizable with coefficients which depend on the strain invariants [29].

The various constant-coefficient nonlinear k - ϵ models bear a striking similarity which allows them to be represented in common form. Each model proposes

$$-\rho \overline{u_i u_j} = -P_t \delta_{ij} + 2 \mu_t E_{ij} - \frac{\mu_t^2}{P_t} C_\beta \left(S_{\beta ij} - \frac{1}{3} S_{\beta mm} \delta_{ij} \right) + \frac{\mu_t^2}{P_t} F_{ij}, \quad (25)$$

where $P_t = 2/3 \rho k$ is the turbulent pressure, $S_{\beta ij}$ represents terms which are quadratic in the mean velocity gradients, C_β is a vector of empirical constants, and F_{ij} is a general, second-order tensor. Summation is performed over β , and so $S_{\beta ij}$ takes three forms:

$$S_{1ij} = \frac{\partial U_i}{\partial x_k} \frac{\partial U_j}{\partial x_k}, \quad S_{2ij} = \frac{1}{2} \left(\frac{\partial U_i}{\partial x_k} \frac{\partial U_k}{\partial x_j} + \frac{\partial U_j}{\partial x_k} \frac{\partial U_k}{\partial x_i} \right), \quad S_{3ij} = \frac{\partial U_k}{\partial x_i} \frac{\partial U_k}{\partial x_j}. \quad (26)$$

The conventional linear k - ϵ model, in which the Reynolds stress is modeled by the Boussinesq approximation, is obtained when C_β and F_{ij} are zero. The major differences in the models can be confined to the trailing term, F_{ij} .

Referring to Table 1, the 1984 model by Yoshizawa included a material derivative of the strain rate and third-order second derivative term, but they were never recommended for use. The 1986 model by Yoshizawa includes a term to model thermal buoyancy effects that was used to obtain good results for the flow over a heated flat plate [28], but it seems to be frequently overlooked by other researchers [7,10].

Speziale's 1987 model includes a material derivative of the strain rate which was felt to be significant in his calculation of the flow over a backward facing step [32], but it has more recently been proven to be unstable. The instability was investigated by the current authors by analogy to the Burnett relation for laminar stress, and the term has been dropped in practice, both by the current authors and by Speziale himself.

The model by Myong and Kasagi includes a term for near-wall effects in a two-dimensional channel. For that term, m and n represent the streamwise and normal directions in the two-dimensional channel, and no summation is performed over them. As a result, the term is not generally applicable [20].

The constants in Eq. (25), listed in Table 1, are empirical. It can be seen that agreement among the various investigators for C_1 and C_3 is fairly good. This may be attributed to the fact that most models were calibrated, either experimentally or computationally, with two-dimensional channel flow in which C_2 does not appear. The agreement on C_2 is very poor, apparently due

to the relative lack of effort spent on its calibration.

Much of the nonlinear k - ϵ modeling effort has focused on two-dimensional problems, such as backward facing steps with and without heat transfer [7,16,30,32,33], heated flat plates [28], combustor flows [13], and rotating channel flows [37,38]. Applications in three-dimensional problems, on the other hand, have been largely unaddressed in the literature. Speziale applied his model in a curved, developing duct flow and expressed optimism over the results [12]; however, the turbulence quantities which were used in the anisotropic eddy viscosity were obtained from experimental data, not from the turbulence equations.

Explicit Algebraic Reynolds Stress Modeling

The similarity between the implicit ARSM and explicit nonlinear k - ϵ models can be easily shown. Toward that end, an approximate solution of the implicit ARSM is obtained by assuming that the Reynolds stress can be represented by the series expansion

$$\tau_{ij} = -P_t \delta_{ij} + A_1 \mu_t E_{ij} + \dots \quad (27)$$

where higher-order terms (squares, cubes, etc.) in E_{ij} and Ω_{ij} , the irrotational and rotational strain rate tensors, are included but not shown. This series expansion is substituted for the Reynolds stresses appearing in Eq. (24), and terms which are higher than second order in the strain rate tensors are subsequently neglected. The resulting expression is

$$\tau_{ij} = -P_t \delta_{ij} + A_1 \mu_t E_{ij} - A_2 \frac{\mu_t^2}{P_t} \left(E_{ik} E_{kj} - \frac{1}{3} \delta_{ij} E_{mn} E_{mn} \right) + A_3 \frac{\mu_t^2}{P_t} \left(E_{ik} \Omega_{kj} + E_{jk} \Omega_{ki} \right) \quad (28)$$

where

$$A_1 = \frac{4(1-\gamma)}{3C_\mu(C_1-1)}, \quad A_2 = A_1^2, \quad \text{and} \quad A_3 = \frac{A_1^2}{2}. \quad (29)$$

It is expected that $A_1 = 2$; however, $C_\mu = .09$, $.6 < \gamma < .78$, and $1.4 < C_1 < 2.2$ imply $A_1 \geq 2.72$. On the other hand, for the purposes of comparison, choosing the values $\gamma = 0.8$ and $C_1 = 2.48$, gives $A_1 \approx 2$, $A_2 \approx 4$, and $A_3 \approx 2$. This explicit form of Rodi's model can also be described using Table 1, where its resemblance to the explicit models discussed above can be seen.

Furthermore, recent research, and the availability of computer-aided symbolic manipulation, have allowed for the *exact* solution of a generalized form of the implicit ARSM, where a range of linear pressure strain models and non-inertial effects are included [8].

The general solution for three-dimensional flow is quite complicated, but in the limit of two-dimensional flow, the solution can be written

$$\begin{aligned}
\tau_{ij} = & -P_t \delta_{ij} + B_1 \mu_t^* E_{ij} - B_2 \frac{\mu_t^{*2}}{P_t} \left(E_{ik} E_{kj} - \frac{1}{3} \delta_{ij} E_{mn} E_{mn} \right) + B_3 \frac{\mu_t^{*2}}{P_t} \left(E_{ik} \Omega_{kj} + E_{jk} \Omega_{ki} \right) \\
& + B_4 \frac{\mu_t^{*2}}{P_t} \left(e_{mjk} \omega_m E_{ik} - e_{mki} \omega_m E_{kj} \right)
\end{aligned} \tag{30}$$

where e_{ijk} is the permutation tensor, and ω_i is the system rotation tensor. The term μ_t^* uses the standard definition for eddy viscosity but with C_μ replaced by C_μ^* which is now a function of the ratio of production to dissipation. (For homogeneous flows in equilibrium, $C_\mu^* \approx .09$.) In addition, each of the four B terms is a constant multiple of

$$B_0 = \frac{3}{3 - 2\eta_1 - 6\eta_2} \tag{31}$$

in which η_1 and η_2 represent scalar functions of the irrotational and rotational strain rate invariants. For example,

$$\eta_1 \propto \left(\frac{k}{\epsilon} \right)^2 E_{mn} E_{mn} \approx \frac{1}{500} \left(\frac{\tau}{T} \right)^2 < 1. \tag{32}$$

The right-hand inequality in Eq. (32) holds for small rates of irrotational strain, or when the time scale of the turbulence is much smaller than the time scale set by the irrotational strain rate. When η_2 is also small, $B_0 \approx 1$. Then, the B terms become constant and can be set, using the Launder, Reece, and Rodi model constants, to be $B_1 \approx 2$, $B_2 \approx 1.25$, $B_3 \approx 1.7$, and $B_4 \approx 6.7$.

Thus, under the assumption of homogeneous turbulence in equilibrium, in the limit of two-dimensional flow and for small rates of strain, the explicit ARSM of Gatski and Speziale can be included in Table 1 in the form of the nonlinear k - ϵ model, where the Launder, Reece, and Rodi model has been used to set the constants.

It is more important, however, to note that for sufficiently large rates of strain, the term in Eq. (31) can become singular. In this explicit form, the term can be regularized so that it is well-behaved in these situations where the model is not formally valid; however, Eq. (31) highlights why the implicit ARSM has been found, at times, to be unstable [8].

Discussion

In summary, while Rodi's implicit ARSM was a major step in anisotropic modeling, the explicit solution of Gatski and Speziale is more convenient and allows for the removal of any inherent singularities. In the limit of two-dimensional flow, the explicit solution reduces to a quadratic form which can be represented by any of the nonlinear k - ϵ models in the limit of small rates of strain. For many flows, these limits are not severe, and so the nonlinear k - ϵ models will capture most of the effects available from the original ARSM.

The current authors, for instance, have obtained improved results for internal duct flows using a constant-coefficient nonlinear k - ϵ model. The average fluctuating velocities in fully-developed two-dimensional channel flow, which would be predicted equal by a linear model, are shown in

Figure 3 compared to experimental data, where it can be seen that the nonlinear model provides considerable improvement. Additionally, the secondary velocities in a fully-developed three-dimensional square duct flow were obtained and are shown in Figure 4. Here, the comparison to data shows that the velocities are much improved in contrast to the zero secondary-velocity that the linear model must give. And while highly three-dimensional flows have remained largely unaddressed in the literature, the current authors have obtained improved normal Reynolds stresses for the flow over a 6:1 prolate spheroid at 10° angle-of-attack, the results of which have been submitted for publication. These results suggest that the nonlinear k - ϵ model gives improvements even in the case of highly three-dimensional flow; however, knowing that nonlinear k - ϵ models represent ARSMs in the limit of *two-dimensional* flow, such applications should be regarded with considerable caution.

For flows of interest to RNS3D, the nonlinear k - ϵ model should offer many advantages. Any of the generic constant-coefficient models should suffice, but particular attention should be paid to the work of Myong and Kasagi [20,21] as it seems to be the only effort to study anisotropic effects in the near-wall region, a region of consequence for the current effort. As mentioned, the near-wall term added by Myong and Kasagi was not frame invariant, but may be suitable under the RNS3D coordinate system or amenable to generalization.

Finally, the model of Shih and Lumley [29], which had not been studied by the current authors until recently, appears to be a viable alternative to the models discussed in more detail here. Clearly, in satisfying realizability, the model becomes slightly more complicated. In any case, the near-wall region would still need separate attention as it has not been addressed by Shih and Lumley [29].

IV. CONCLUSIONS AND RECOMMENDATIONS

Conclusions

The current effort has incorporated a two-equation k - ϵ model with low-Reynolds number modifications in order to address deficiencies in RNS3D in the prediction of duct flows with vortex generators. Coding and implementation is entirely consistent with RNS3D coding and assumptions, which will allow NASA LeRC personnel already familiar with the code some flexibility with regards to modifications. The equations appear to be efficient in solving a circular pipe flow and capture the near-wall region well.

Proposed Future Activity

The goal of improving the capability of NASA LeRC personnel in predicting the turbulence quantities in duct flows with vortex generators has been largely realized in the current effort. The RNS3D code now includes a more general two-equation turbulence model applicable in the near-wall region, and it exists in a form which will be familiar to RNS3D users. Future efforts should include careful examination of the coding to additional applications to ensure that the model is made suitably robust. The ability of NASA LeRC personnel to use the new model will greatly expedite that process.

Nonlinear k - ϵ models, such as those proposed by Yoshizawa (1984) [35] and Speziale (1987) [30], have become an attractive option to users of the k - ϵ model, and more recent work by Gatski and Speziale has shown the extent to which these constant coefficient, explicit nonlinear models anticipated the solution of the implicit algebraic models such as that by Rodi [8]. But it has also shown that the models only formally apply in the limit of two-dimensional flow. In addition, while most models do not take the near-wall region into account, work by Myong and Kasagi [20] includes a near-wall term which, with slight modification, may be suitable for use in duct flows controlled by vortex generators. Because the RNS3D code now includes a two-equation model, the step to include anisotropic effects becomes a relatively minor one, and its implementation should be included in any future activity.

REFERENCES

1. ANDERSON, B.H., HUANG, P.S., PASCHAL, W.A., & CAVATORTA, E. 1992 The Design Strategy for the Re-Engining Modification of the 727-100 Center Inlet Duct Including Vortex Flow Control Using CFD. *AIAA Paper No. 92-0152*.
2. ARMFIELD, S.W. & FLETCHER, C.J. 1989 Comparison of $k-\epsilon$ and Algebraic Reynolds Stress Models for Swirling Diffuser Flow. *Int. Journal for Num. Methods in Fluids*. **9**, 987-1009.
3. BOGER, D.A., McDONALD, H., & SHIEH, C.M. 1995 Duct Flows with Vortex Generators, A Final Technical Report for NASA-LeRC Grant NAG3-1485.
4. BRILEY, W.R., & McDONALD, H. 1984 Three-Dimensional Viscous Flows with Large Secondary Velocity. *J. Fluid Mech.* **144**, 47-77.
5. CHIEN, K.-Y. 1982 Predictions of Channel and Boundary-Layer Flows with a Low-Reynolds-Number Turbulence Model. *AIAA Journal*. **20** (1), 33-38.
6. DEMUREN, O. & RODI, W. 1984 Calculation of Turbulence-Driven Secondary Motion in Non-Circular Ducts. *J. Fluid Mech.* **140**, 189-222.
7. DUTTA, S. & ACHARYA, S. 1993 Heat Transfer and Flow Past a Backstep with the Nonlinear $k-\epsilon$ Turbulence Model and the Modified $k-\epsilon$ Turbulence Model. *Numerical Heat Transfer A*. **23**, 281-301.
8. GATSKI, T.B. & SPEZIALE, C.G. 1993 On Explicit Algebraic Stress Models for Complex Turbulent Flows. *J. Fluid Mech.* **254**, 59-78.
9. GESSNER, F.B. & JONES, J.B. 1965 On Some Aspects of Fully-Developed Turbulent Flow in Rectangular Channels. *J. Fluid Mech.* **23**, 689-713.
10. HAROUTUNIAN, V. 1994 Progress in Simulating Industrial Flows Using Two-Equation Models: Can More Be Achieved with Further Research? *NASA CP 10165*, 155-169.
11. HREYNYA, C.M., BOLIO, E.J., CHAKRABARTI, D., & SINCLAIR, J.L. 1995 Comparison of Low Reynolds Number $k-\epsilon$ Turbulence Models in Predicting Fully Developed Pipe Flow. *Chem. Eng. Sci.* **50** (12), 1923-1941.
12. HUR, N., THANGAM, S. & SPEZIALE, C.G. 1990 Numerical Study of Turbulent Secondary Flows in Curved Ducts. *J. Fluids Eng.* **112**, 205-211.

13. HWANG, C.C., ZHU, G., MASSOUDI, M. & EKMANN, J.M. 1993 A Comparison of the Linear and Nonlinear k - ϵ Turbulence Models in Combustors. *J. Fluids Eng.* **115**, 93-102.
14. JONES, W.P. & LAUNDER, B.E. 1972 The Prediction of Laminarization with a Two-Equation Model of Turbulence. *Int. J. Heat Mass Transfer.* **16**, 1119-1130.
15. KIM, K.Y. & CHUNG, M.K. 1988 Calculation of a Strongly Swirling Turbulent Round Jet with Recirculation by an Algebraic Stress Model. *Int. J. Heat and Fluid Flow.* **9** (1), 62-68.
16. KOBAYASHI, T., MORINISHI, Y. & TOGASHI, S. 1993 Estimation of Anisotropic k - ϵ Model on the Backward-Facing Step Flow by LES Data Base. *J. Wind Eng. Ind. Aero.* **46** & **47**, 77-84.
17. KOLLMANN, W., ed. 1980 *Prediction Methods for Turbulent Flows*. von Karman Institute.
18. LAUNDER, B.E., & SHARMA, B.I. 1974 Application of the Energy-Dissipation Model of Turbulence to the Calculation of Flow Near a Spinning Disc. *Letters in Heat and Mass Transfer.* **1**, 131-138.
19. LUMLEY, J.L. 1970 Toward a Turbulent Constitutive Relation. *J. Fluid Mech.* **41**, 413-434.
20. MYONG, H.K. & KASAGI, N. 1990 Prediction of Anisotropy of the Near-Wall Turbulence With an Anisotropic Low-Reynolds-Number k - ϵ Turbulence Model. *J. Fluids Eng.* **112**, 521-524.
21. MYONG, H.K. & KOBAYASHI, T. 1991 Prediction of Three-Dimensional Developing Turbulent Flow in a Square Duct With an Anisotropic Low-Reynolds-Number k - ϵ Model. *Trans. ASME.* **113**, 608-615.
22. NISIZIMA, S. 1989 Numerical Study of Turbulent Square-Duct Flow Using an Anisotropic k - ϵ Model. *Trans. Japan Soc. Mech. Eng. B.* **55** (512), 991-998.
23. NISIZIMA, S. & YOSHIZAWA, A. 1987 Turbulent Channel and Couette Flows Using an Anisotropic k - ϵ Model. *AIAA Journal.* 414-420.
24. RIVLIN, R.S. 1957 The Relation Between the Flow of Non-Newtonian Fluids and Turbulent Newtonian Fluids. *Q. App. Math.* **15** (2), 212-215.
25. RODI, W. 1976 A New Algebraic Relation for Calculating the Reynolds Stresses. *ZAMM.* **56**, T219-T221.
26. RODI, W. 1982 Examples of Turbulence Models for Incompressible Flows. *AIAA Journal.* **20** (7), 872-879.

27. RUBINSTEIN, R. & BARTON, J.M. 1990 Nonlinear Reynolds Stress Models and the Renormalization Group. *Phys. Fluids A*. **2** (8), 1472-1476.
28. SADA, K. & ICHIKAWA, Y. 1993 Simulation of Air Flow over a Heated Flat Plate Using Anisotropic k - ϵ Model. *J. Wind Eng. Ind. Aero.* **46 & 47**, 697-704.
29. SHIH, T-H, ZHU, J., & LUMLEY, J.L. 1995 A New Reynolds Stress Algebraic Equation Model. *Comput. Methods Appl. Mech. Engrg.* **125**, 287-302.
30. SPEZIALE, C.G. 1987 On nonlinear K - l and K - ϵ Models of Turbulence. *J. Fluid Mech.* **178**, 459-475.
31. SPEZIALE, C.G. 1994 A Review of Reynolds Stress Models for Turbulent Shear Flows. *20th Symposium on Naval Hydrodynamics*. University of California, Santa Barbara.
32. SPEZIALE, C.G. & NGO, T. 1988 Numerical Solution of Turbulent Flow Past a Backward Facing Step Using a Nonlinear k - ϵ Model. *Int. J. Eng. Sci.* **26** (10), 1099-1112.
33. THANGAM, S. & SPEZIALE, C.G. 1992 Turbulent Flow Past a Backward-Facing Step: A Critical Evaluation of Two-Equation Models. *AIAA Journal*. **30** (5), 1314-1320.
34. WARFIELD, M.J. & LAKSHMINARAYANA, B. 1987 Computation of Rotating Turbulent Flow with an Algebraic Reynolds Stress Model. *AIAA Journal*. **25** (7), 957-964.
35. YOSHIKAWA, A. 1984 Statistical Analysis of the Deviation of the Reynolds Stress from its Eddy-Viscosity Representation. *Phys. Fluids*. **27**, 1377-1387.
36. YOSHIKAWA, A. 1986 Statistical Modeling of Turbulent Thermally Buoyant Flows. *J. Phys. Soc. Japan*. **55** (9), 3066-3072.
37. YOUNIS, B.A. 1990 Prediction of Flows in Rotating Non-Circular Ducts with a Two-Equation Model of Turbulence. *ASME FED*. **103**, 115-122.
38. YOUNIS, B.A. 1993 Prediction of Turbulent Flows in Rotating Rectangular Ducts. *Trans. ASME*. **115**, 646-652.
39. ZHONG, X., MacCORMACK, R.W. & CHAPMAN, D.R. 1993 Stabilization of the Burnett Equations and Application to Hypersonic Flows. *AIAA Journal*. **31** (6), 1036-1043.

Table 1: A Comparison of Nonlinear k - ϵ Models

Model	C_1	C_2	C_3	F_{ij}
Yoshizawa (1984)	2.37	-0.393	1.98	$-5.14 \frac{DE_{ij}}{Dt} + 7.43 \frac{\mu_t}{\rho} \frac{\partial^2 E_{ij}}{\partial x_k \partial x_k}$
Speziale (1987)	3.36	2.24	-1.12	$4.48 \frac{DE_{ij}}{Dt}$
Nisizima, Yoshizawa (1987)	5.76	?	-1.23	0
Yoshizawa (1986)	5.76	-16.5	-1.23	$-2.47\gamma \left(g_i \frac{\partial T}{\partial x_j} + g_j \frac{\partial T}{\partial x_i} - \frac{2}{3} g_k \frac{\partial T}{\partial x_k} \delta_{ij} \right)$
Nisizima (1989)	4.69	-27.2	-0.551	0
Rubinstein, Barton (1990)	2.80	17.1	-1.15	0
Myong, Kasagi (1990)	5.93	3.33	-1.11	$4.94 \frac{\mu}{\mu_t} \left(\delta_{ij} + \delta_{in} \delta_{jn} - 4\delta_{im} \delta_{jm} \right) \left(\frac{\partial \sqrt{k}}{\partial x_n} \right)^2$
Sada, Ichikawa (1993)	4.69	-27.2	-0.551	$2.47 \frac{Gr}{Re^2} \left(\delta_{ij} \frac{\partial T}{\partial x_j} + \delta_{j\beta} \frac{\partial T}{\partial x_i} - \frac{2}{3} \delta_{k\beta} \frac{\partial T}{\partial x_k} \delta_{ij} \right)$
Burnett (1935)	1.86	1.68	-0.172	$-2.03 \frac{DE_{ij}}{Dt} - .341\gamma \left(g_i \frac{\partial T}{\partial x_j} + g_j \frac{\partial T}{\partial x_i} - \frac{2}{3} g_k \frac{\partial T}{\partial x_k} \delta_{ij} \right)$
Rodi (1976)*	2.02	2.02	0	0
Gatski, Speziale (1993)*	1.18	.625	-0.550	$6.725 (E_{ik} e_{mjk} \Omega_m - e_{mki} \Omega_m E_{kj})$

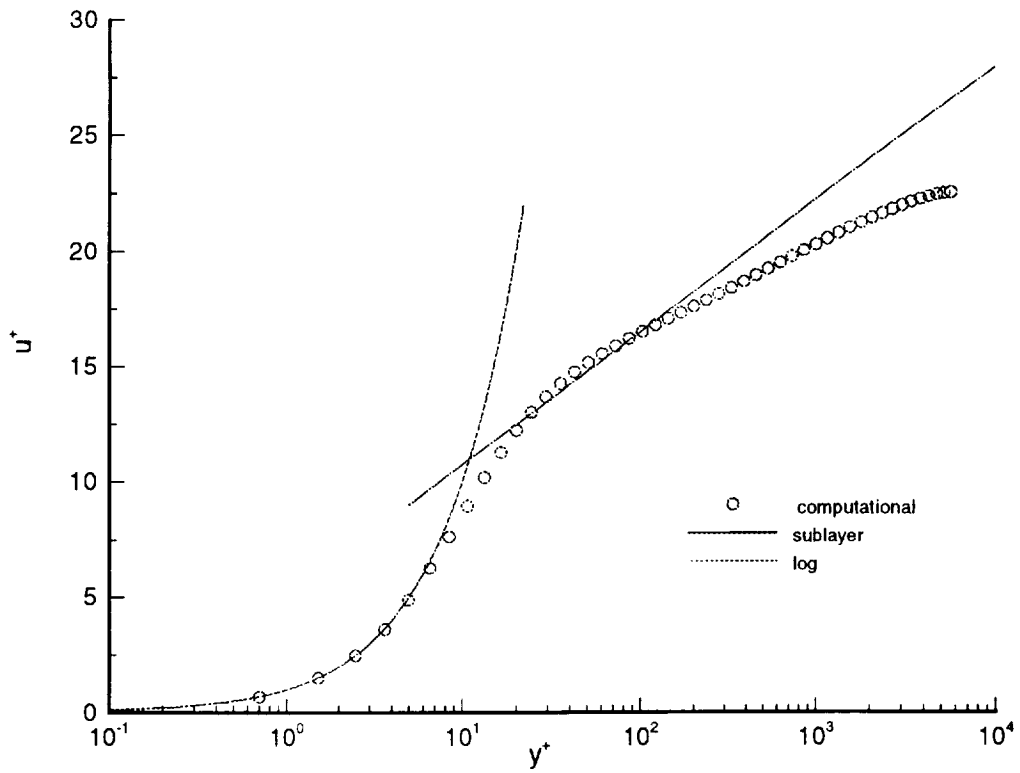


Figure 1. Velocity Profile for Fully-Developed Pipe Flow, $Re=150,000$

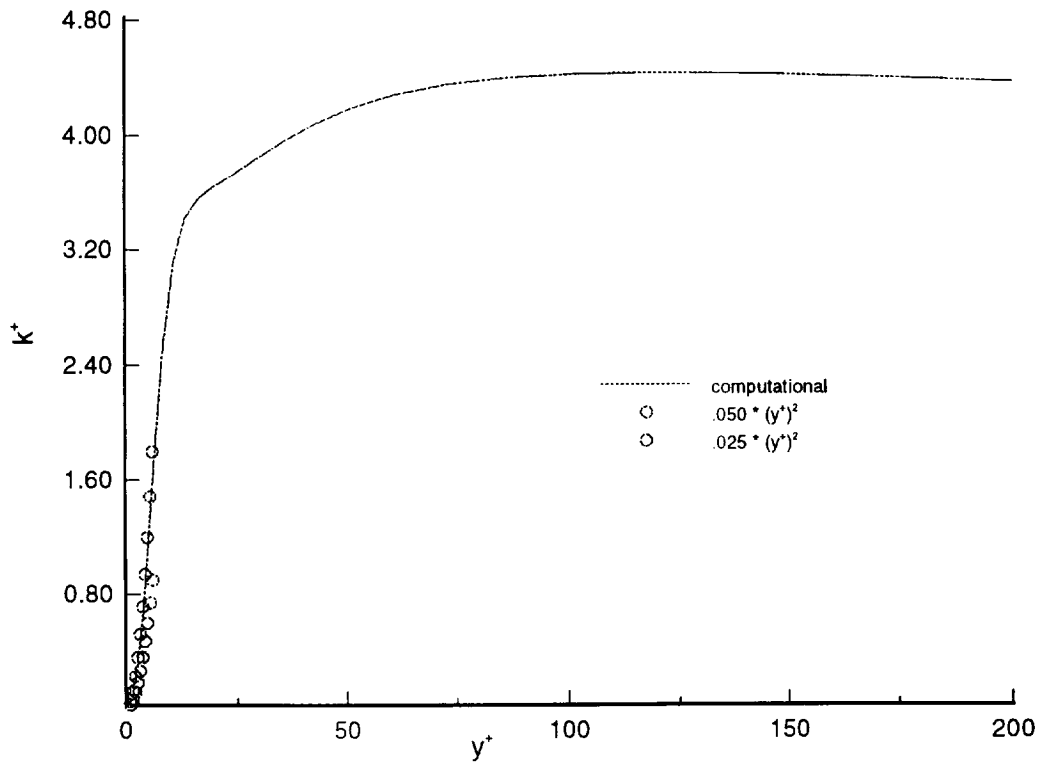


Figure 2. Near-Wall Turbulent Kinetic Energy Profile, $Re=150,000$

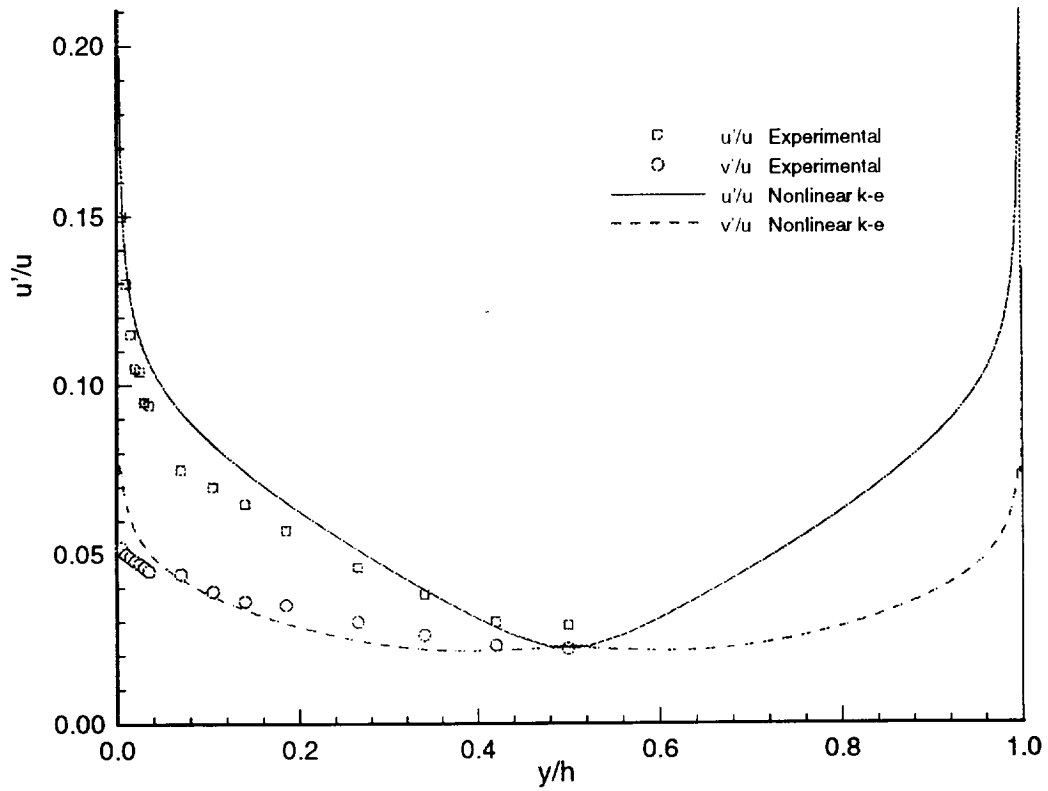


Figure 3. Fluctuating Velocities in a Two-Dimensional Channel, $Re=150,000$

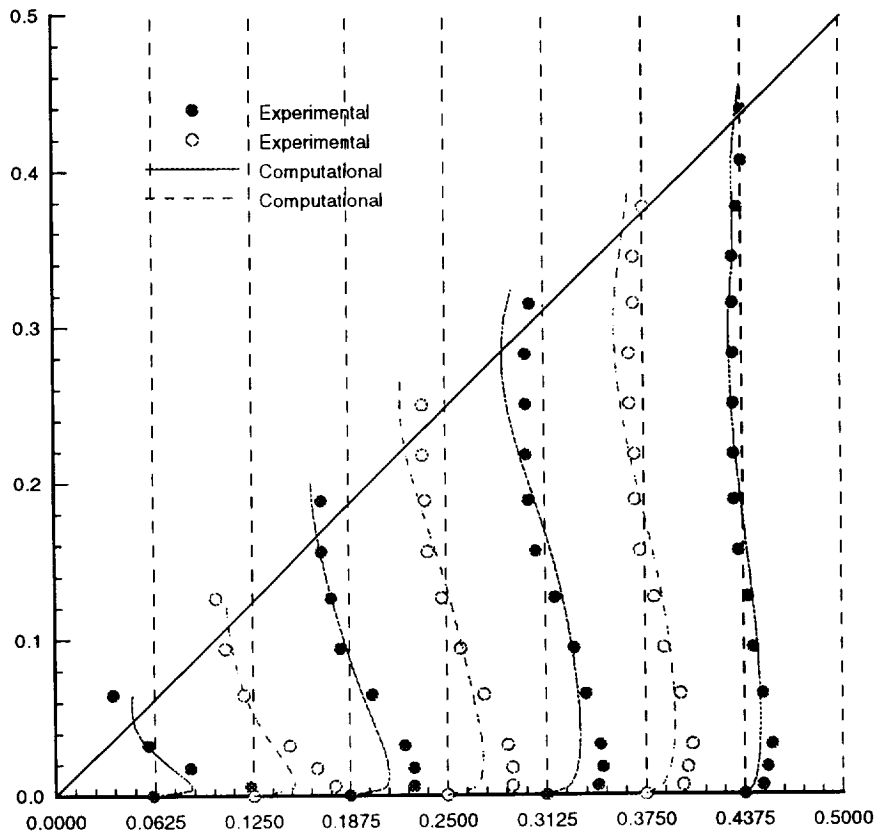


Figure 4. W / U_0 Profiles in the Square Duct, $Re=150,000$